Frequency dispersion of electro-optical properties over a wide range by means of time-response analysis

Mustapha Abarkan, Jean-Paul Salvestrini, Michel Aillerie, Marc Fontana

Frequency dispersion of electro-optical properties over a wide range by means of time-response analysis

Mustapha Abarkan, Jean Paul Salvestrini, Michel Aillerie, and Marc D. Fontana

We show that a Z-transform-based time-response analysis of the electro-optical response of a crystal to a step voltage with a short rise time allows one to obtain the dispersion of the electro-optical coefficients over a wide frequency range. We describe the method employed and present the results obtained for the main electro-optic coefficients (r_{22}, r_{61}, and r_c) of a standard $LiNbO_3$ crystal. We also show that this method is able to provide even small values of the electro-optic coefficients as well as the dispersion within a wide frequency range, which is limited only by the rise time of the step voltage.

1. Introduction

For the design of electro-optical (EO) devices such as modulators or Q-switch Pockels cells, the frequency dispersion over a wide frequency range of the EO coefficients for the crystal used in the device is one of the most important characteristics that should be known or determined. It is well established[1,2] that several processes contribute to the total EO effect. In particular, if the crystal is piezoelectric, the contributions are different when the frequency of the applied electric field is below or above the acoustic resonances of the crystal. Below these piezoresonances, the crystal is free to deform, and the variation of the strain follows the applied electric field on the basis of the inverse piezoelectric effect. Subsequently, the corresponding birefringence change (via the elasto-optic effect) leads to an indirect contribution to the EO coefficient measured at constant stress T and denoted ${r_{ijk}}^T$. If the frequency of the applied electric field is well above the frequencies of the acoustic resonances, the crystal is unable to deform itself and is thus virtually clamped, so that the EO coefficient, corresponding to the direct EO effect, is measured at constant strain S and denoted ${r_{ijk}}^S$. The difference between ${r_{ijk}}^T$ and ${r_{ijk}}^S$, owing to the indirect EO effect, arises from the contribution of acoustic phonons and can be estimated by the product of the components $p_{ijmn} \times d_{mnk}$ of the elasto-optic $\mathbf{p}$ and piezoelectric $\mathbf{d}$ tensors, respectively. At resonance frequencies, some EO coefficients can be greatly enhanced. The knowledge of the amplitude of the acoustic phonon contributions and their values at resonance frequencies are needed and used to build resonant EO modulators, with the advantage of a lower driving voltage. Indeed the half-wave voltage V_π, allowing 100% of modulation, could be divided by 10 or even more because the EO coefficients are enlarged at these particular frequencies. As the amplitude of the resonance is proportional to the product $p_{ijmn} \times d_{mnk}$, a large acoustic phonon contribution is thus required and often desired in EO modulators. However, it should be noted that, in general, the acoustic resonances constitute a drawback in the case of an EO Q-switch in that they lead to an unwanted reduction in output energy and to multiple output pulses.[3]

The techniques mainly used for the measurements of the EO coefficients' dispersion[4] in bulk materials are based on the amplitude-modulation depth of a laser beam, which passes through the sample under test, induced by a sinusoidal electric field with varying frequency. Because the values of the EO coefficients are generally small, a large amplitude of the electric field is usually required to achieve a sufficient signal-to-noise ratio and thus to ensure a good accuracy in the measurement of the EO coefficients' values. Unfortunately, the frequency bandwidths of

The authors are with the Laboratoire Matériaux Optiques, Photonique et Systèmes, Formation de Recherche en Evolution Centre Nationale de la Recherche Scientifique 2304, Université de Metz et Supélec, 2, rue E. Belin, 57070 Metz, France. The e-mail address of J. P. Salvestrini is salvestr@ese-metz.fr.

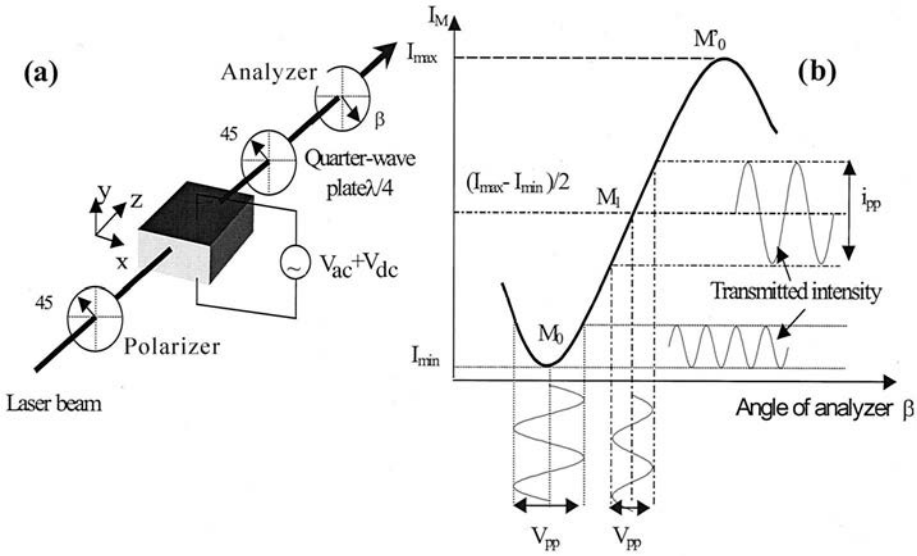

Fig. 1. (a) Sénarmont arrangement used for EO measurements. (b) Optical transmission function versus the angle of the analyzer β. The point M_0 is the minimum transmission point for which the output optical signal has a frequency twice as big as the frequency of the applied electric field. M_1 is the 50% transmission point yielding the linear replica of the ac voltage.

the voltage generators, delivering a voltage in the kilovolt range, are limited to a few tens of kilohertz. As a consequence, the above techniques can be used only in the low-frequency range, generally under acoustic resonance frequencies. It is thus often impossible to separate the acoustic contributions from the whole response.

We propose here a novel, to our knowledge, technique that is based on a typical EO-modulation configuration and that allows the frequency range in the EO measurements to be extended to at least 150 MHz. A prior version of this technique was proposed by R. Spreiter *et al.*[5] and implemented successfully in an interferometer, for the EO characterization of a new organic crystal by use of a relatively small voltage (<100 V). These authors showed that it was possible to obtain easily the different contributions to the large EO coefficient r_{11} of this crystal.

We present here a comprehensive study and a more extended analysis of the technique in question that we have implemented in the Sénarmont setup and use voltage varying to as much as 1000 V. The method consists of the measurement of the time response of the EO crystal when subjected to a step voltage. The step voltage is obtained by our switching a large voltage (to as much as 1 kV) in a short time (a few nanoseconds). Coupled with the *Z*-transform analysis of the optical signal, this kind of voltage supply, combined with an efficient optical detection system, allows the measurement of the EO coefficients' dispersion on a bulk crystal over a wide frequency range. By this method, the various contributions of the EO properties corresponding to the indirect and direct EO coefficients could be determined at the same time, with a good accuracy even for small values of EO coefficients.

In the following, the new method under consideration is presented and applied to the standard $LiNbO_3$ crystal. The results of the measurements of the r_{22}, r_{61}, and r_c coefficients are given, discussed, and compared with those obtained with more classical methods. We first describe the experimental setup used in this study and the two usual techniques (in the low-frequency range) generally employed for the EO characterizations of bulk crystals. These well-mastered methods, based on the amplitude modulation, are used here to check the consistency, at low frequencies, with the results obtained by our new technique, which is called time-response method (TRM). This new method is then presented with its experimental setting conditions, the analysis of the EO time response to an electric step voltage, and the mathematical treatment necessary to obtain the frequency response.

2. Experimental Setup and Low-Frequency Methods

The classical Sénarmont setup commonly used for EO measurements is shown in Fig. 1(a). As can be seen, the sample is sandwiched between a polarizer and a quarter-wave plate, the neutral axes of which are oriented at 45° from the axes of the crystal. The incident light beam goes through a linear polarizer oriented at 45° from the axes of the crystal and then through the EO crystal that induces a differential phase shift. Behind the quarter-wave plate, a rotating analyzer allows one to measure the variations of the phase shift induced by the applied electric field or by other external factors, such as a mechanical stress or temperature variations.[6] As the crystal and any other component of the setup are not optically perfect, the contrast $\gamma = (I_{\max} - I_{\min})/(I_{\max} + I_{\min})$ at the output of the setup is not, in general, equal to unity.

Within this consideration, the equation of the

transfer function of the light intensity transmitted through the setup [Fig. 1(b)] can be written as[7]:

$$T = \frac{1 - \gamma \sin(\Gamma - 2\beta)}{2}, \tag{1}$$

where β and Γ are the angular position of the analyzer and the phase shift introduced by the EO crystal, respectively. Usually, the contrast γ is considered a constant parameter, and only the phase shift Γ is supposed to be sensitive to the applied electric field E according to the equation

$$\Gamma(E) = \frac{2\pi L}{\lambda} \Delta n(E), \tag{2}$$

where L is the length of the crystal along the beam propagation direction, λ is the laser wavelength, and $\Delta n(E)$ is

$$\Delta n(E) = \Delta n_0 - \tfrac{1}{2} n_{\text{eff}}{}^3 r_{\text{eff}} E. \tag{3}$$

In this equation, Δn_0 is the intrinsic birefringence (without the applied electric field) and n_{eff} and r_{eff} are the effective refractive index and the effective EO coefficient, respectively.

At point M_0 [Figure 1(b)], at which the transmitted intensity is minimum (i.e., $I = I_{\min}$), an alternative electric field of frequency ν, applied to the EO crystal, generates an optical signal modulated at the double frequency 2ν. This working point is often used to determine the static EO coefficient.[6] The double-frequency signal is lost as a step of a dc electric field is applied to the crystal and can be recovered if the analyzer is rotated by an angle given by

$$\Delta\beta = \frac{\Delta\Gamma}{2} = \frac{\pi L}{2\lambda} n^3 r_{\text{eff}} E. \tag{4}$$

This first technique is called the frequency-doubling method (FDM).

The point M_1 of the transfer function [Fig. 1(b)] corresponds to the 50% transmission $[(I_{\max} - I_{\min})/2]$ point. The so-called linear working point M_1 is associated with the modulation-depth method (MDM) and can be used to determine the EO coefficient as a function of frequency. Measuring the peak-to-peak amplitude i_{pp} of the modulated signal at the point M_1, one can obtain the EO coefficient directly from the following equation[7]:

$$r_{\text{eff}}(\nu) = \frac{2\lambda D}{\pi n_{\text{eff}}{}^3 I_0 L} \frac{i_{\text{pp}}(\nu)}{V_{\text{pp}}(\nu)}. \tag{5}$$

Here $I_0 = I_{\max} - I_{\min}$ represents the total intensity shift of the transfer function, D is the sample thickness along the applied electric field direction, and V_{pp} is the peak-to-peak value of the applied ac field at the frequency ν. It is to be pointed out that the relationship described by Eq. (5) is an approximation valid only for applied voltages over which the transmission curve can be considered linear.

It should be mentioned that, for both the FDM and the MDM, only the absolute value of the EO coefficient is determined. Nevertheless, in the case of the MDM, the relative change of the sign of the EO coefficient is, as we will see below, revealed by a change in the phase shift between electrical and optical signals.

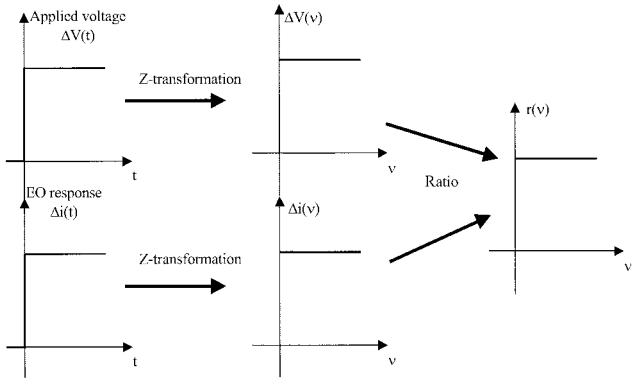

Fig. 2. Calculus sequences for obtaining the frequency response of the EO coefficients. The applied voltage has a step form.

3. Step-Voltage Time-Response Method

The M_1 point can be also used to obtain the time dependence of the EO response. At this working point, the instantaneous variation of the transmitted beam intensity $\Delta i(t)$ induced by the applied voltage $\Delta V(t)$ is given by

$$\Delta i(t) = \frac{\pi n_{\text{eff}}{}^3 L I_0}{2\lambda D} r_{\text{eff}}(t) \otimes \Delta V(t), \tag{6}$$

where $\otimes$ is the convolution operator and $r_{\text{eff}}(t)$ is the instantaneous value of the EO coefficient.

As we can display and measure on an oscilloscope the time signals $\Delta i(t)$ and $\Delta V(t)$, the frequency dispersion of the EO coefficients can be derived (see Fig. 2) from the ratio of $\Delta i(\nu)$ and $\Delta V(\nu)$, which are obtained by the Z transformation of the signals $\Delta i(t)$ and $\Delta V(t)$, respectively,

$$r_{\text{eff}}(\nu) = \frac{2\lambda D}{\pi n_{\text{eff}}{}^3 I_0 L} \frac{\Delta i(\nu)}{\Delta V(\nu)}. \tag{7}$$

To determine the above Z transforms, we consider $\Delta i(t)$ and $\Delta V(t)$ as discrete functions $\Delta i(t_n)$ and $\Delta V(t_n)$ of N samples taken within a period T. Within these considerations, the time interval between successive samples $\Delta\tau = (T/N)$ and the sampling time t_n are linked to each other by the equation

$$t_n = n\Delta\tau. \tag{8}$$

The Z transform of the signals $\Delta i(t)$ and $\Delta V(t)$ is given by

$$\Delta i(\nu_m) = \sum_{n=0}^{N-1} Z^{-n} \Delta i(t_n), \qquad \Delta V(\nu_m) = \sum_{n=0}^{N-1} Z^{-n} \Delta V(t_n), \tag{9}$$

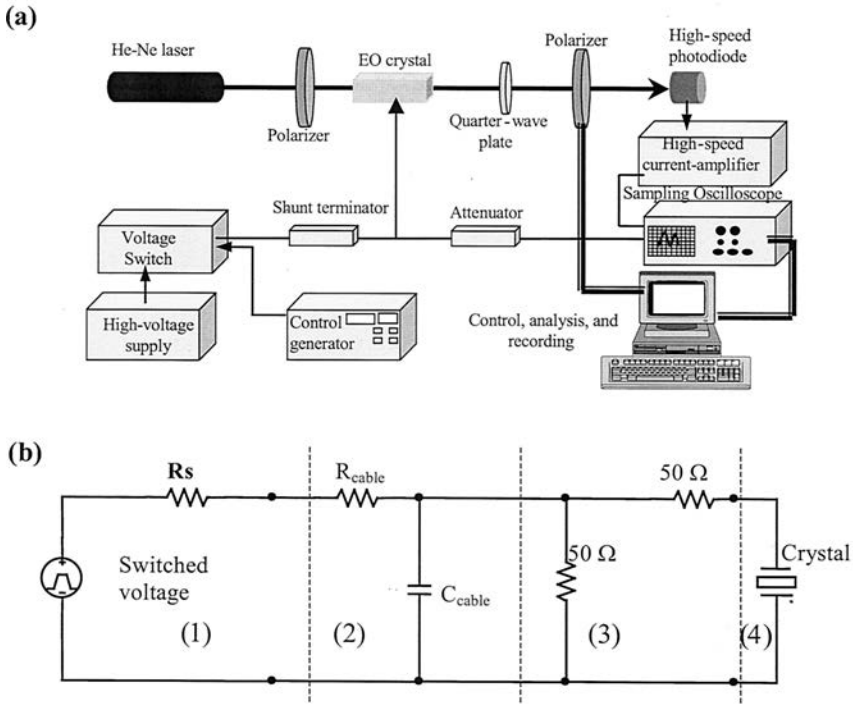

Fig. 3. (a) Schematic diagram of the experimental setup for measuring EO time response. (b) Equivalent circuit of the electrical part of the experimental setup: (1) pulse generator, (2) electric cable, (3) shunt terminator, and (4) crystal.

with $m = 0, \ldots, N$ and $\nu_m = m/T$, where ν_m is the frequency at data number m and Z is written as

$$Z = \exp\left(-2i\pi \frac{m}{N}\right). \tag{10}$$

The first advantage of this method, based on the analysis of the EO response to the application of a step voltage, is that the contribution coming from acoustic phonons is included in the response, provided that the temporal width of the step is large enough. The second advantage concerns the wider EO frequency range $\nu_{\max}$ achievable by this method, owing to the possibility of reducing to a few nanoseconds the rise time of the step voltage. Nevertheless, note that care must be taken for the driving voltage so that the voltage rising edge (which carries all the high frequencies) is not broadened or reflected.

4. Experimental Results and Discussion

Figure 3(a) depicts the electrical and optical arrangement used for the implementation of this new method with the devices and apparatus described as follows.

The applied voltage consists of a 0–1000-V dc power supply and a high-voltage switch (HV 1000 model from DEI), ensuring a rise time lower than 10 ns (depending on the capacitance of the load). This switch is driven by a pulse generator (PM/5715 Philips model), the pulse duration of which can reach the value of 10 μs with a rise time of 6 ns.

To avoid the broadening or the reflection of the voltage rising edge, we took care to match the output impedance of the pulse generator (50 Ω) to the supplying cable and to the crystal load. For this purpose, we have connected the output of the voltage switch to the crystal via a 50-Ω cable with a length as short as possible, and then we have provided the crystal with a 50-Ω shunt terminator [see Fig. 3(b)].

The detection system consists of a high-speed p-i-n photodiode having 1 mm^2 of active surface and a response time lower than 0.5 ns, combined with a voltage-current amplifier having a response time equal to 0.8 ns and a transimpedance gain equal to 2.10^4 V/A. A sampling oscilloscope, with a sampling rate of 10 GSa/s and an analogical bandwidth of 500 MHz, displays the applied voltage and the detected optical signal with a response time equal to 0.7 ns.

We have performed measurements on the well-known and widely studied $LiNbO_3$ crystal grown with the Czochralski technique from a congruent melt (48.5 mol.% LiO_2 and 51.5 mol.% Nb_2O_5). We have used three samples cut in a parallelepipedic shape to explore three different configurations involving the EO coefficients r_{22}, r_{61}, and r_c. For each sample the dimension along the light beam propagation is 40 mm, and the interelectrode thickness is 3 mm for configurations involving the coefficients r_{22} and r_{61} and 5 mm for the configuration r_c. Table 1 summarizes the configurations (directions of the light propagation and the applied electric field and EO coefficient involved) that were studied.

A. Low-Frequency Measurements: Results with the Frequency-Doubling and Modulation-Depth Methods

The measurements were carried out at room temperature with a He–Ne laser (λ = 633 nm). For the

Table 1. Description of the Electro-Optical Configurations Used in Our Experiments on Lithium Niobate Crystals[a]

Symmetry–EO Tensor	Configuration	EO Coefficient
3m	$\mathbf{E}//z$ $\mathbf{k}//x$ or y	$r_c = r_{33} - \left(\frac{n_0}{n_e}\right)^3 r_{13}$
$\begin{bmatrix} 0 & -r_{22} & r_{13} \\ 0 & r_{22} & r_{13} \\ 0 & 0 & r_{33} \\ 0 & r_{42}=r_{51} & 0 \\ r_{51} & 0 & 0 \\ r_{61}=-r_{22} & 0 & 0 \end{bmatrix}$	$\mathbf{E}//y$ $\mathbf{k}//z$	r_{22}
	$\mathbf{E}//x$ $\mathbf{k}//z$	r_{61}

[a] x, y, and z are the principal dielectric axes of the crystal, and $\mathbf{k}$ and $\mathbf{E}$ designate the light beam propagation and the applied electric field directions, respectively.

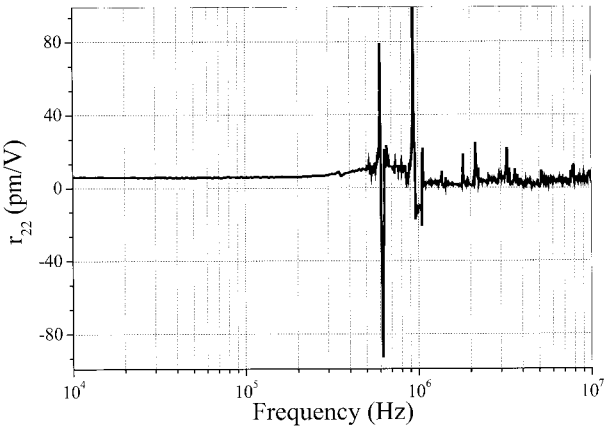

Fig. 5. Frequency dispersion of the EO coefficient r_{22} obtained via the MDM measurements in $LiNbO_3$.

FDM and the MDM, we used an ac voltage of 150-V peak to peak and a dc voltage amplitude varying between 0 and 500 V. To illustrate the results of the measurements with the FDM, we plot in Fig. 4 an example of the recorded phase shift Γ (involving the r_c coefficient) as a function of a dc voltage V applied along the z axis and for a light propagating along the x axis. It should be mentioned that Γ is a relative phase shift, and thus we have arbitrarily fixed its value equal to zero for a voltage equal to 0 V. As expected, the induced phase shift is proportional to the applied voltage, and the slope of the curve allows, by use of Eq. (4), the determination of the static absolute value of the r_c coefficient, which is found to be equal to $|r_c| = 20.3$ pm/V (see Table 2).

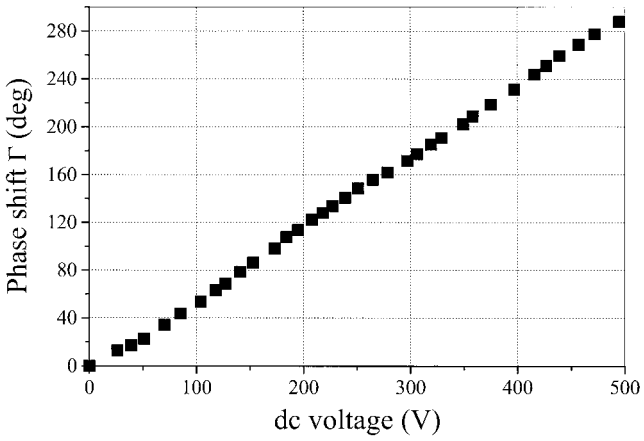

Fig. 4. Phase shift Γ (involving the EO coefficient r_c) induced by a dc voltage applied along the z axis for a light beam propagating along the x axis.

Figure 5 shows the frequency dispersion of the EO coefficient r_{22} as obtained via the MDM measurements. The frequency of the applied voltage is varied from 1 kHz to 10 MHz. Each point of the curve is calculated, with Eq. (5), from the measurement of the amplitude of the induced modulated signal. We also have taken into account the relative phase between the optical and the electrical signals. This could reveal possible changes of relative sign of the EO coefficient with the frequency of the applied electric field. We can distinguish two parts in this dispersion curve. In the low-frequency part, the value of the coefficient r_{22} is constant below 500 kHz and is equal within experimental errors to the static one ($|r_{22}| = 6.4$ pm/V), which has been obtained by the FDM (see Table 2). Above 500 kHz, the EO behavior exhibits several acoustic resonances for which the coefficient reaches large values and changes of its relative sign. This change is due to the fact that, at these particular frequencies, the crystal becomes conductive, giving rise to a variation of the imaginary part of the refractive index (electroabsorption). This change induces a phase shift between the electrical and the optical signals, leading to a change of sign of the EO coefficient when the value of the phase shift is equal to 180 deg. The different frequencies that are observed in Fig. 5 correspond to different vibrational

Table 2. Absolute Values of EO Coefficients at Constant Stress (r^T) and at Constant Strain (r^S) in $LiNbO_3$ Obtained at 633 nm and at Room Temperature by Various Techniques[a]

	r^T (pm/V)				r^S (pm/V)	
Coefficient	FDM	MDM	TRM (long time period)	Literature	TRM (short time period)	Literature
$\lvert r_{22}\rvert$	6.6 ± 0.2	6.4 ± 0.3	6.4 ± 0.3	6.4[9]	3.8 ± 0.2	3.4[8]
$\lvert r_{61}\rvert$	6.1 ± 0.3	6 ± 0.3	6 ± 0.3	6.5[10]	3.6 ± 0.2	—
$\lvert r_c\rvert$	20.3 ± 0.8	19.7 ± 1.1	19.7 ± 1.1	19.9[11]	19.7 ± 1.1	18[8]

[a] Owing to symmetry consideration, the values of the EO coefficients r_{22} and r_{61} have to be equal.

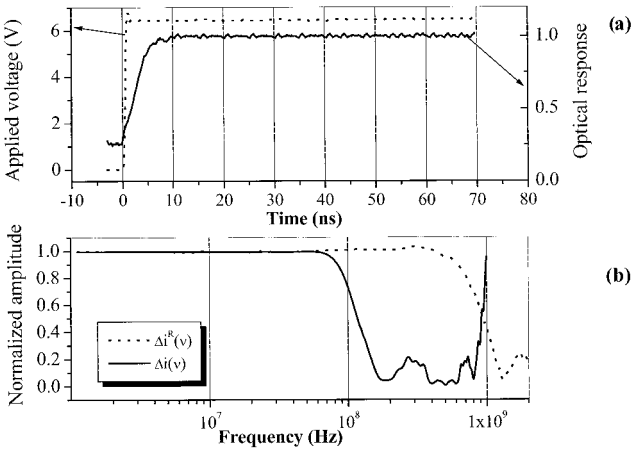

Fig. 6. (a) Time response of the optical detector and of the applied step voltage. (b) The deduced response $\Delta i(\nu)$ of the detection system and the ideal response $\Delta i^R(\nu)$.

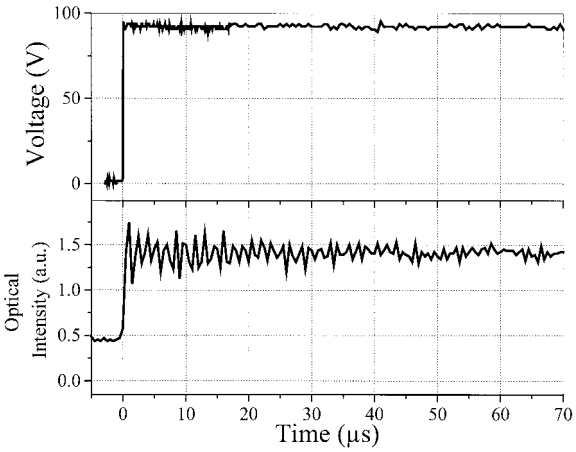

Fig. 7. Plots versus time of the applied voltage and the optical signal for the configuration involving the EO coefficient r_{22}.

acoustic modes of the sample and their harmonics. Indeed, according to the crystal dimensions, the acoustic resonances probably occur to as much as a few tens of megahertz. This frequency region is not directly reachable with conventional voltage amplifiers at the high-voltage range, and therefore a clear determination of the clamped EO coefficient is not possible. As a consequence, it is difficult to deduce accurately the acoustic contribution to the EO properties from data plotted in Fig. 5 and thus to obtain the high-frequency values of the coefficient r_{22}. To overcome this limitation and thus to increase the frequency range of the EO measurements, we will now analyze the results that we obtained with the step-voltage EO response.

B. Time-Response Measurements: Results with the Time-Response Method

At first, to obtain the frequency bandwidth of the optical detection, we used the setup and the method with the sample of $LiNbO_3$ prepared for the r_c configuration (see Table 1). We took care to replace the step generator with a faster one that has a rise time equal to 1 ns but a smaller voltage (6.5 V). Thanks to the rather large value of the EO coefficient r_c, this weak voltage induced a modulation depth of 3%, which is a value just sufficient to be detected. Figure 6(a) shows both the applied step voltage and the corresponding optical response obtained in this case. After normalization and Z transformation via Eq. (9) of the data depicted in Fig. 6(a), we obtain the frequency response of the system [Fig. 6(b)]. This result represents, in fact, the response $h(\nu)$ of the optical detector itself in that the EO coefficient r_c is known to be constant from 0 to several gigahertz, without any jump around piezoelectric resonances, and in that the rise time of the step generator is shorter than that of the optical detection system. The function $h(\nu)$ is given by the following relation:

$$h(\nu) = \frac{\Delta i(\nu)}{\Delta i^R(\nu)}, \tag{11}$$

where $\Delta i(\nu)$ is the measured response of the detection system and $\Delta i^R(\nu)$ is the ideal step response. Using Eq. (11), we can rewrite Eq. (7) to take into account the detection response:

$$r_{\text{eff}}(\nu) = \frac{2\lambda d}{\pi n_{\text{eff}}^3 I_0 L} \frac{\Delta i(\nu)}{\Delta V(\nu) h(\nu)}. \tag{12}$$

According to Fig. 6(b), we can consider that, in this case, the frequency bandwidth of our experimental setup is approximately 150 MHz. At higher frequencies the signal coming from the detection system is not properly induced by the electric field but is due to noise only.

Figure 7 shows the recording of both the applied voltage and the optical signal measured for the configuration involving the EO coefficient r_{22}. In this case, the amplitude of the step voltage is 90 V, and its rise time is equal to 6 ns. These results were obtained after appropriate signal processing including high-frequency noise filtering and temporal shift suppression (this temporal shift resulted from the different lengths of the electrical wires). Owing to the large interaction length (40 mm) between the light beam and the electric field in the sample, such a small voltage was adequate to achieve a sufficiently high signal-to-noise ratio. The main period of the oscillations generated by the acoustic resonances that appear in the optical response curve of Fig. 7 corresponds to the frequency (600 kHz) of the first large peak that appears on the curve showing the frequency dispersion of the EO coefficient (Fig. 5). A more detailed analysis of the data plotted in Fig. 7 shows the existence of a second oscillation of the signal that is superimposed on the first one. The period of this second signal corresponds to the frequency of the second main resonance appearing in Fig. 5, which is equal to 940 kHz. For long time periods, above 70 μs (not plotted on Fig. 7), the oscillations are completely damped, and the optical response remains constant. The insets of Fig. 8 illustrate the EO response in the case of the coefficient r_{22} for two time scales. For time periods shorter than 200 ns, the

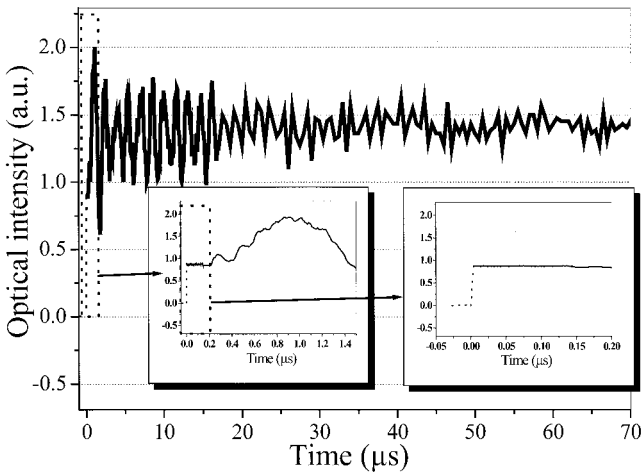

Fig. 8. Time dependence at different time scales of the optical signal for the configuration involving the EO coefficient r_{22} of $LiNbO_3$. For time periods shorter than 1 ns, the solid curves are replaced by dotted curves and are only guidelines for the eyes.

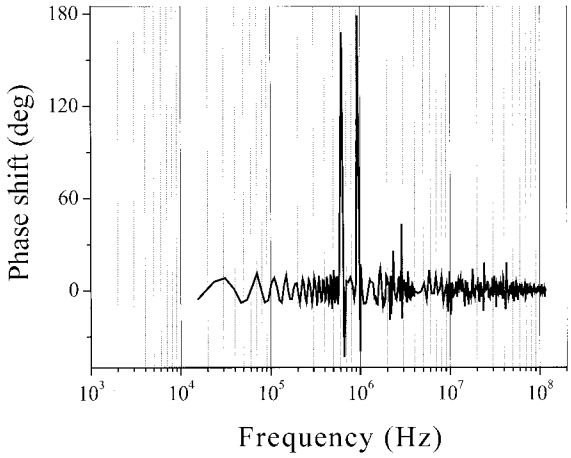

Fig. 10. Deduced phase shift (by use of the Z transformation) between the applied step voltage and the optical response, corresponding to the difference of the arguments of $\Delta i(\nu)$ and $\Delta V(\nu)$. The sign of the EO coefficient is positive if the phase is zero and negative if the phase is equal to 180 deg.

oscillations do not exist because the acoustic waves need more time to propagate across the crystal. The value of the intensity corresponding to the plateau appearing for time periods below 200 ns is much smaller than that obtained for time periods larger than 70 μs, which indicates a large acoustic contribution.

By use of Eq. (12) and application of the mathematical treatment described above in Eqs. (6)–(10) to the data plotted in Fig. 7, it is now possible to determine the frequency dispersion of the coefficient r_{22}. This dependence, as derived from the TRM measurements, is shown and compared with the directly measured (MDM) data in Fig. 9. The maximum duration of the pulse (a few tens of microseconds), which was used in the TRM measurements, leads to a limitation, as seen in Fig. 9(b), in the low-frequency range to a frequency equal to 15 kHz. Both methods give consistent results. The calculated (TRM) and the direct experimental values (MDM) of r_{22} are equal for frequencies below the resonances (see Table 2), and the main resonances appear at the same frequencies. Above 10 MHz and to as much as 150 MHz, the coefficient r_{22} remains constant with an absolute value of 3.8 pm/V. This value is in good agreement with that reported in Ref. 8, which was measured at a frequency of 100 MHz. Figure 9 shows a significant discrepancy between results deduced from the TRM and MDM in the acoustic resonance frequency range. As we have seen above, the sign of the measured values of the coefficient r_{22} obtained via the MDM changes when a resonance frequency is encountered. This is not the case with the results obtained via the TRM, for which the sign of the coefficient remains positive in the whole frequency range. This is due to the fact that we did not take into account the arguments of $\Delta i(\nu)$ and $\Delta V(\nu)$ when we calculated $r_{22}(\nu)$ using Eq. (12). This approximation is valid only for frequencies below and above resonances in that in these ranges the arguments should present the same values. This is not the case in the megahertz-frequency range in which the acoustic resonances occur. Here the difference of the arguments of $\Delta i(\nu)$ and $\Delta V(\nu)$ should also be close to zero except for resonance frequencies, for which the difference should be close to 180 deg, leading then to an opposite sign of r_{22}. This assertion is confirmed by data plotted in Fig. 10. The calculated phase, corresponding to the difference of the arguments of $\Delta i(\nu)$ and $\Delta V(\nu)$, could be assumed to be, apart from noise, equal to zero in the whole frequency range, except around the two resonance frequencies (600 and 940 kHz), at which the phase changes to approximately 180 deg and thus induces a change in the sign of the coefficient r_{22}.

More generally, it is pointed out in Table 2 that the three methods give reliable results because they provide consistent values for each EO coefficient. More-

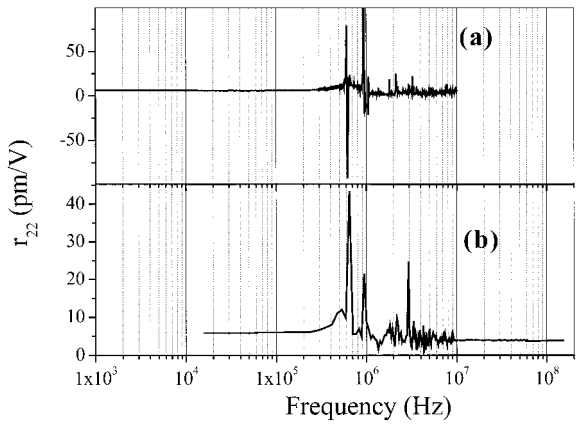

Fig. 9. Comparison in the frequency dispersion of the EO coefficient r_{22} of $LiNbO_3$ between (a) direct values obtained by measurements within the MDM and (b) values derived from the TRM.

Table 3. Comparison between the Difference $|r^T - r^S|$ Derived from our Measurements and the Product of $p \times d$ in $LiNbO_3$[a]

EO Coefficient	$\lvert r^T - r^S \rvert$ (pm/V)	$\lvert p \times d \rvert$ (pm/V)	Corresponding Acoustic Contributions
r_{22}	2.6 ± 0.3	2.6	$(p_{11} - p_{12})d_{22} - p_{14}d_{15}$
r_{61}	2.4 ± 0.3	2.6	$(p_{11} - p_{12})d_{22} - p_{14}d_{15}$
r_c	~0	0.4	$[p_{33} - (n_0/n_e)^3 p_{13}]d_{33} + [2p_{31} - (n_0/n_e)^3 (p_{11} + p_{12})]d_{31}$

[a]The values of the **d** and **p** coefficients come from Ref. 12 and 13, respectively.

over, these results are in good agreement with those reported in literature.[9–11]

In addition, we have checked the validity of our results by comparing the acoustic phonon contribution, represented by the difference between the constant stress r^T and the constant strain r^S measured values of the EO coefficient, with the product $\mathbf{p} \times \mathbf{d}$[1,2] of the components of the elasto-optic and piezoelectric tensors, respectively. Table 3 summarizes the results of this comparison and shows the good agreement, within experimental errors, between the acoustic contribution derived from our measurements and those calculated via the combination of the elasto-optic and piezoelectric effects.[12,13]

5. Conclusion

We have presented a new technique to measure EO coefficients, which is based on an analysis of the EO response to an appropriate step voltage. We have shown that this method allows one to obtain the frequency dispersion of the EO coefficient within a wide frequency range, which is limited only by the voltage-switching time. This new technique gives the possibility of separating the different contributions to the EO effect and especially allows discrimination between clamped and unclamped coefficients.

Because the amplitude of the switched step voltage could be large (several kilovolts), the technique is suitable even for the measurement of small values of EO coefficients. Indeed, we have successfully applied the method to measuring the small EO coefficient r_{22} in the beta-barium borate crystal, using a sample with a small interaction length ($L = 5$ mm). We have found a value of 2 ± 0.1 pm/V (without any dispersion in the frequency range to as much as 150 MHz), which is in good agreement with the literature.[14] Owing to its large sensitivity, the present technique is useful for the determination of the value of the acoustic contribution of the EO coefficient even if it is small. Thus, for instance, the acoustic contribution was easily measured and found to be equal to only 1 pm/V in the organic–inorganic 2A5NPDP crystal.[15]

We are grateful to Katalin Polgar (Research Institute for Solid State Physics and Optics of the Hungarian Academy of Sciences, Budapest, Hungary) for supplying lithium niobate and beta-barium borate crystals. We thank Nicophorous Theofanous for interesting discussions and his critical reading of the manuscript. This work was supported by the Région Lorraine and the Ministère de la Recherche in the framework of the Contrat de Plan Etat Région.

References

1. A. Yariv and P. Yeh, "Physical properties of electro-optic coefficient," in *Optical Waves in Crystals*, (Wiley, New York, 1984) pp. 264–266.
2. J. P. Salvestrini, M. D. Fontana, B. Wyncke, and F. Brehat, "Comparative measurements of the frequency dependence of electro-optical and dielectric coefficients in inorganic crystals," Nonlinear Opt. **17,** 271–280 (1997).
3. P. C. Amundsen and G. Wang, "Low-loss $LiNbO_3$ *Q*-switches: compensation of acoustically-induced refractive index variations," IEEE J. Quantum Electron. **23,** 2252–2257 (1987).
4. M. Aillerie, M. D. Fontana, and N. Théofanous, "Measurement of electro-optic coefficients: description and comparison of the experimental techniques," Appl. Phys. B **70,** 317–334 (2000).
5. R. Spreiter, Ch. Bosshard, F. Pan, and P. Gûnter, "High-frequency response and acoustic phonon contribution of the linear electro-optic effect in DAST," Opt. Lett. **22,** 564–566 (1997).
6. M. Aillerie, M. D. Fontana, F. Abdi, C. Carabatos-Nedelec, N. Théofanous, and G. E. Alexakis, "Influence of the temperature-dependent spontaneous birefringence in the electro-optic measurements of $LiNbO_3$," J. App. Phys. **65,** 2406–2408 (1989).
7. L. Guilbert, J. P. Salvestrini, M. D. Fontana, and H. Hassan, "Combined effects due to phase, intensity, and contrast in electro-optic modulation: application to ferroelectric materials," IEEE J. Quantum. Electron. **35,** 273–280 (1999).
8. A. Chirakadze, S. Machavariani, A. Natsvlishvili, and B. Hvitia, "Dispersion of the linear electro-optic effect in lithium niobate," J. Phys. D **23,** 1216–1218 (1990).
9. F. Abdi, M. Aillerie, P. Bourson, M. D. Fontana, and K. Polgar, "Electro-optic properties in pure $LiNbO_3$ crystals from the congruent to the stoichiometric composition," J. Appl. Phys. **84,** 2251–2254 (1998).
10. M. Aillerie, F. Abdi, M. D. Fontana, N. Théofanous, and E. Abarkan, "Accurate measurements of the electro-optic coefficients and birefringence changes using an external modulation signal," Rev. Sci. Instrum. **70,** 1627–1634 (2000).
11. E. H. Turner, "High frequency electro-optic coefficients of lithium niobate," Appl. Phys. Lett. **8,** 303–304 (1966).
12. A. W. Warner, M. Onoe, and G. A. Coquin, "Determination of elastic and piezoelectric constants for crystals in class (3m)," J. Acoust. Soc. Am. **46,** 1223–1231 (1966).
13. R. W. Dixon and M. G. Cohen, "A new technique for measuring magnitudes of photoelastic tensors and its application to lithium niobate," Appl. Phys. Lett. **8,** 205–207 (1966).
14. C. A. Ebbers, "Linear electro-optic effect in β-BaB_2O_4," Appl. Phys. Lett. **52,** 1948–1949 (1988).
15. J. Zaccaro, J. P. Salvestrini, A. Ibanez, P. Ney, and M. D. Fontana, "Electric-field frequency dependence of Pockels coefficients in 2-amino-5-nitropyridium dihydrogen phosphate organic–inorganic crystals," J. Opt. Soc. Am. B **17,** 427–432 (2000).